UDC 629.5.015

Ivo SENJANOVIĆ
Neven HADŽIĆ
Nikola VLADIMIR

Restoring Stiffness in the Hydroelastic Analysis of Marine Structures

Review paper

The restoring stiffness, that couples displacements and deformations, plays very important role in hydroelastic analysis of marine structures. The problem of its formulation is quite complex and is still discussed in the relevant literature. In the paper, the recent formulations of restoring stiffness are correlated and analyzed. Due to some equivalent terms of the restoring and geometric stiffness as a result of common load, the unified stiffness is established and compared with the complete restoring stiffness known in the relevant literature. It is found out that the new formula deals with more terms, and, that under some assumptions, it is reduced to the known complete restoring stiffness. The unified stiffness constitution is analyzed through derived analytical formulae for prismatic pontoon. Its consistency is checked for the rigid body displacements. Also, numerical results of the hydroelastic response of segmented barge are correlated with available model test results. Some issues, that are important for practical implementation in the hydroelastic code for flexible structures, are described.

Keywords: *geometric stiffness, hydroelasticity, restoring stiffness, segmented barge*

Povratna krutost u hidroelastičnoj analizi pomorskih konstrukcija

Pregledni rad

Povratna krutost, koja spreže pomake i deformacije, igra važnu ulogu u hidroelastičnoj analizi pomorskih konstrukcija. Njezino formuliranje predstavlja složen problem i još je uvijek predmet rasprave u stručnoj literaturi. U ovom članku aktualne formulacije povratne krutosti uspoređene su i analizirane. Zbog nekih ekvivalentnih članova povratne i geometrijske krutosti kao rezultata zajedničkog opterećenja, postavljena je sjedinjena krutost i uspoređena s ukupnom povratnom krutosti poznatom u literaturi. Ustanovljeno je da nova formula ima više članova, a uvođenjem odgovarajućih pretpostavki reducirana je na poznati oblik kompletne povratne krutosti. Konstitucija sjedinjene krutosti analizirana je putem izvedenih analitičkih formula za prizmatičan ponton. Njezina konzistencija provjerena je na primjeru krutoga tijela. Također, numerički rezultati hidroelastičnog odziva segmentne barže uspoređeni su s dostupnim rezultatima modelskog ispitivanja. Navedene su i neke upute za implementaciju izvedenog algoritma u program za hidroelastičnu analizu pomorskih konstrukcija.

Ključne riječi: *geometrijska krutost, hidroelastičnost, povratna krutost, segmentna barža*

Authors' Address (Adresa autora):
University of Zagreb, Faculty of Mechanical Engineering and Naval Architecture,
Ivana Lučića 5, 10 000 Zagreb, Croatia
E-mail: ivo.senjanovic@fsb.hr

Received (Primljeno): 2010-05-14
Accepted (Prihvaćeno): 2010-10-10
Open for discussion (Otvoreno za raspravu): 2012-10-01

1 Introduction

Recent trends in increasing vessel size and speed on one hand and optimization of ship structure on the other result in a quite flexible ship hull. Natural vibrations of such ships can easily fall into resonance with the encounter frequency in an ordinary sea state. Large container ships are a special subject of investigation since they are particularly sensitive to quartering seas due to reduced torsional stiffness caused by large hatch openings [1].

The ship response is usually classified as springing or whipping, depending on steady-state or transient nature of vibrations. Great effort is put into investigation of fluid-structure interaction both from extreme loading and fatigue point of view, which are important for ship structure design and safety [2].

The ship hydroelastic analysis includes definition of structural model, mass distribution, restoring stiffness, added mass, damping and wave excitation [3]. In spite of the fact that ship hydroelasticity has been a known subject for many years [4] some questions remain open. Constitution of restoring stiffness, which is not as straightforward as one could imagine, is one of them [5].

Basically, there are two approaches, a pure hydromechanical one and another that extends to the structure. Within the former approach, in the well-known Price and Wu formulation, only the basic hydrostatic pressure term is considered [6]. Newman formula represents an extension, giving the necessary hydrostatic pressure coefficients [7]. However, neither of those two formulations gives the complete restoring stiffness coefficients for the rigid body motions because the gravity part is missing.

The above shortcoming is removed by Riggs [8], specifying new modal pressure coefficients and adding the gravity term, in the form shown in Table 1, Eq. (1). The index notation and

summation convention is used for compactness, where X, Y and Z are global coordinates; h is the natural mode (rigid or elastic); S is the wetted surface; n is the unit normal vector to the wetted surface; ρ, ρ_S , are the fluid and structure mass densities, and g is gravity constant.

A further improvement is done by Huang and Riggs [9], offering a combined hydroelastic and structural formulation of restoring stiffness, Eq. (2) in Table 1, where σ_{kl} is stress tensor due to gravity and hydrostatic loads. The last integral in Eq. (2) actually represents the well-known geometric stiffness matrix.

The next two identical expressions, which are obtained in different way, are given by Malenica and Molin, [10, 11], Eq. (3) in Table 1. The first one is based on the variational principle, while the latter is derived by employing vector differential and integral calculus [12].

The last column in Table 1, Eq. (4), represents the formulation based on variational principle, [13]. First the energy of involved forces is estimated and then it is varied per displacement and mode amplitude. The same expressions are obtained indirectly by specializing the general formula, Eq. (2), for rigid body motion [14]. However, in the source equation (4), [13], both rigid body and elastic modes are equally valuated. This quite important fact is commented later on. In [14] some other transformations of general formula, Eq. (2), related to Eqs. (1), (3) and (4), are also derived and discussed. That is more interesting from theoretical than practical point of view.

The unit normal vector to the wetted surface in [8, 9] is directed into the fluid. In order to make comparison of different restoring stiffness formulations easier, sign of n_k in Eqs. (1) and (2) in Table 1 is changed. Based on experience and comparison of different known formulations, shown in Table 1 in a systematic way, the following conclusions can be drawn:

1. Stiffness is defined as a relation between force and displacement. The generalized force is marked with index i and therefore in the restoring stiffness definition the same index must be added to modal displacement, and not to deformation, i.e. derivatives.
2. Eq. (4) satisfies this basic condition, which ensures the convergence of transfer function of bending moment to zero as encounter frequency approaches zero value [13].
3. Eq. (1) has the same items as Eq. (4) but with opposite mode indices i and j on the corresponding quantities in all three terms, that according to Point 1 is not correct and consequently leads to an error in transfer functions.
4. Similar situation is with Eq. (3). The mode variation term in C_{ij}^{nh}, Eq. (3b), as well as C_{ij}^{m}, Eq. (3d), have opposite mode indices i and j than those in Eq. (4), that also results with some discrepancies [13]. This is an implication of mixing of displacement variation and its gradient.
5. Eq. (2) includes geometric stiffness into the complete restoring stiffness. It is shown in [9] that k_{ij}^{G} contains gravity stiffness C_{ij}^{m}, Eq. (4d), so that it does not explicitly occur in the formulation. On the other side, an additional term, k_{ij}^{SO}, as a contribution from the boundary stress distribution, appears. The same quantities in the common terms of Eqs. (2) and (4), i.e. C_{ij}^{p} and C_{ij}^{nh}, are marked with indices i and j respectively.

The objective of the paper is to derive complete restoring stiffness for slender marine structures in a transparent way, comprising geometric stiffness, Eq. (2e), and consistent restoring stiffness for ships, Eq. (4), and compare it with the known one, Eq. (2). In addition, the intention is to derive the complete restoring stiffness for a pontoon analytically, in order to illustrate the constituting process and make physical meaning of each term recognizable.

2 Modal restoring stiffness

2.1 Hydrostatic stiffness

The restoring stiffness consists of hydrostatic and gravity parts. In order to specify the former, it is necessary to determine the work of pressure in going from the initial wetted surface position $S(\mathbf{r})$ to the instantaneous position $\tilde{S}(\tilde{\mathbf{r}})$, where $\mathbf{r}$ is the position vector, $\tilde{\mathbf{r}} = \mathbf{r} + \mathbf{H}$, and $\mathbf{H}$ is the displacement vector. The pressure work is difference between two potentials

$$W^h = \tilde{P}(\tilde{\mathbf{r}}) - P(\mathbf{r}), \tag{5}$$

which are scalar functions of the vector variables. Similarly to the Taylor series expansion in vicinity of a given point, one can write by neglecting small terms of higher order

Table 1 **Actual formulations of modal restoring stiffness**
Tablica 1 **Aktualne formulacije modalne povratne krutosti**

		Eq. (1)	Eq. (2)	Eq. (3)	Eq. (4)
Contribution from	Notation	Riggs [8]	Huang and Riggs [9]	Malenica, Molin [10, 11]	Senjanović et al. [13], Riggs [14]
a) Pressure	C_{ij}^{p}	$\rho g \iint_S h_i^l h_k^l n_k \mathrm{d}S$ (1a)	$\rho g \iint_S h_k^l h_3^l n_k \mathrm{d}S$ (2a)	$\rho g \iint_S h_k^l h_3^l n_k \mathrm{d}S$ (3a)	$\rho g \iint_S h_k^l h_3^l n_k \mathrm{d}S$ (4a)
b) Normal vector and mode	C_{ij}^{nh}	$\rho g \iint_S Z h_{i,j}^l h_k^l n_k \mathrm{d}S$ (1b)	$\rho g \iint_S Z h_k^l h_{i,j}^l n_k \mathrm{d}S$ (2b)	$\rho g \iint_S Z h_k^l \left(h_{i,j}^l n_k - h_{i,k}^l n_i\right) \mathrm{d}S + \rho g \iint_S Z h_{k,j}^l h_i^l n_k \mathrm{d}S$ (3b)	$\rho g \iint_S Z h_k^l h_{i,j}^l n_k \mathrm{d}S$ (4b)
c) Boundary stress (rigid body)	$-k_{ij}^{SO}$		$-\rho g \iint_S Z h_i^l h_{k,j}^l n_k \mathrm{d}S$ (2c)		
d) Gravity load	C_{ij}^{m}	$g \iiint_V \rho_s h_{3,k}^l h_k^l \mathrm{d}V$ (1d)		$g \iiint_V \rho_s h_{3,k}^l h_k^l \mathrm{d}V$ (3d)	$g \iiint_V \rho_s h_k^l h_{3,k}^l \mathrm{d}V$ (4d)
e) Geometric stiffness	k_{ij}^{G}		$\iiint_V \sigma_{kl} h_{m,k}^l h_{m,j}^l \mathrm{d}V$ (2e)		

$$\tilde{P}(\tilde{\mathbf{r}}) = P(\mathbf{r}) + D_H\left(P(\mathbf{r})\right), \tag{6}$$

where D_H is directional derivative in the way of displacement vector **H**. Thus, Eq. (5) is reduced to

$$W^h = D_H\left(P(\mathbf{r})\right), \tag{7}$$

and since

$$P(\mathbf{r}) = -\rho g \iint_S Z\mathbf{H}\mathbf{n}\mathrm{d}S \tag{8}$$

where $Z = Z(x,y)$ is the vertical coordinate of the wetted surface *S* and **n** is its unit normal vector in the coordinate system used in hydroelastic analysis, Figure 1, yields

$$W^h = -\rho g \iint_S \left[D_H(Z)\mathbf{H}\mathbf{n} + ZD_H(\mathbf{H})\mathbf{n} + Z\mathbf{H}D_H(\mathbf{n})\right]\mathrm{d}S. \tag{9}$$

where

$$D_H(Z) = (\mathbf{H}\nabla)Z = H_z, \quad D_H(\mathbf{H}) = (\mathbf{H}\nabla)\mathbf{H}, \quad D_H(\mathbf{n}) = (\mathbf{H}\nabla)\mathbf{n}, \tag{10}$$

and ∇ is the Hamilton operator. Determination of $D_H(\mathbf{n})$ according to definition Eqs. (10) is not convenient since it requires calculation of normal vector derivatives. Therefore, it is more rational to use the inverse version obtained from the continuum mechanics [15], in which the displacement derivatives are involved, Appendix A. Thus, one finds the following identity equation

$$\mathbf{H}D_H(\mathbf{n}) = \mathbf{H}\mathbf{n}(\nabla\mathbf{H}) - \mathbf{n}(\mathbf{H}\nabla)\mathbf{H}, \tag{11}$$

where the second term in Eq. (11) contains the mode directional derivative, Eqs. (10). Thus, substituting Eq. (11) into Eq. (9) yields

$$W^h = -\rho g \iint_S \left[H_z + Z(\nabla\mathbf{H})\right]\mathbf{H}\mathbf{n}\mathrm{d}S. \tag{12}$$

According to definition, the force is relation between incremental work and displacement, so it is determined from the variational equation, assuming constant force within a small displacement.

$$\delta W^h = -\rho g \iint_S \left[H_z + Z(\nabla\mathbf{H})\right]\delta\mathbf{H}\mathbf{n}\mathrm{d}S. \tag{13}$$

Due to reasons of numerical reduction, the modal superposition method is used, and the variation is transmitted to modes

$$\delta W^h = \sum_{j=1}^{N} \delta W_j^h, \quad \mathbf{H} = \sum_{j=1}^{N} \xi_j \mathbf{h}_j, \quad \delta\mathbf{H} = \sum_{j=1}^{N} \mathbf{h}_j \delta\xi_j. \tag{14}$$

i.e. generalized forces W_j^h and mode ξ_j amplitudes.

In that way, Eq. (13) is decomposed into modal equations

$$\delta W_i^h = -\sum_{j=1}^{N}\left[\left(C_{ij}^p + C_{ij}^{nh}\right)\xi_j\right]\delta\xi_i, \tag{15}$$

where

$$C_{ij}^p = \rho g \iint_S \mathbf{h}_i h_z^j \mathbf{n}\mathrm{d}S, \quad C_{ij}^{nh} = \rho g \iint_S Z\mathbf{h}_i(\nabla\mathbf{h}_j)\mathbf{n}\mathrm{d}S \tag{16}$$

are the modal stiffness coefficients due to pressure, and normal vector and mode contributions, respectively.

2.2 Gravity stiffness

Similarly to the pressure part, Eqs. (8), (9) and (10), the work of gravity force reads

$$W^m = D_H\left[-g\iiint_{\tilde{V}} \rho_s H_z \mathrm{d}V\right] = -g\iiint_V \rho_s(\mathbf{H}\nabla)H_z\mathrm{d}V, \tag{17}$$

where ρ_s and *V* are structure density and volume, respectively.

In order to obtain consistent variational equation, it is necessary to strictly follow the definition of generalized force and to vary displacement vector in Eq. (17) and not its gradient. Thus,

$$\delta W^m = -g\iiint_V \rho_s(\delta H\nabla)H_z\mathrm{d}V. \tag{18}$$

Application of modal superposition method leads to the modal variational equation

$$\delta W_i^m = -\sum_{j=1}^{N} C_{ij}^m \xi_j \delta\xi_i, \tag{19}$$

where

$$C_{ij}^m = g\iiint_V \rho_s(\mathbf{h}_i\nabla)h_z^j\mathrm{d}V \tag{20}$$

are the gravity stiffness coefficients.

Figure 1 **Coordinate system in hydroelastic analysis**
Slika 1 **Koordinatni sustav u hidroelastičnoj analizi**

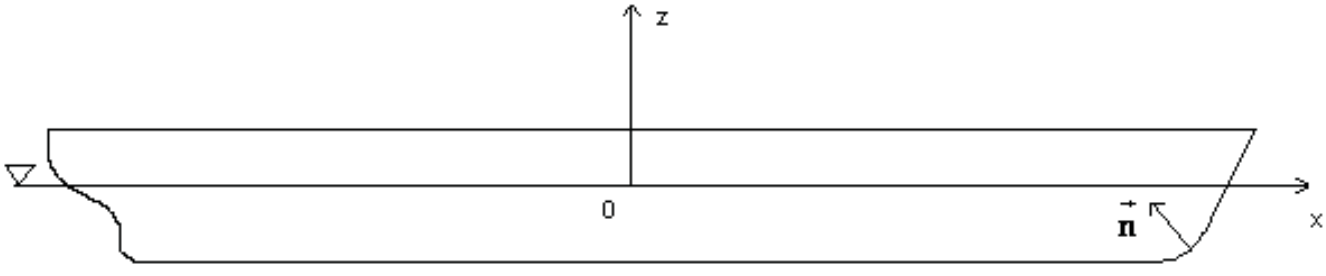

2.3 Restoring stiffness

Finally, the complete restoring stiffness coefficients are obtained by summing up their constitutive parts,

$$C_{ij} = C_{ij}^{p} + C_{ij}^{nh} + C_{ij}^{m}, \tag{21}$$

where in the expanded form

$$C_{ij}^{p} = \rho g \iint_{S} \left(h_x^i n_x + h_y^i n_y + h_z^i n_z \right) h_z^j \mathrm{d}S \tag{22}$$

$$C_{ij}^{nh} = \rho g \iint_{S} Z \left(h_x^i n_x + h_y^i n_y + h_z^i n_z \right) \left(\frac{\partial h_x^j}{\partial x} + \frac{\partial h_y^j}{\partial y} + \frac{\partial h_z^j}{\partial z} \right) \mathrm{d}S \tag{23}$$

$$C_{ij}^{m} = g \iiint_{V} \rho_s \left(h_x^i \frac{\partial h_z^j}{\partial x} + h_y^i \frac{\partial h_z^j}{\partial y} + h_x^i \frac{\partial h_z^j}{\partial z} \right) \mathrm{d}V. \tag{24}$$

The above expressions can be also written in index notation, as stated in Table 1, Eq. (4).

3 Modal structural stiffness

3.1 Governing formulae

Structural stiffness consists of conventional stiffness and geometric stiffness. Both are determined from the basic formulae of the theory of elasticity and continuum mechanics. Despite the fact that structural stiffness is well-known in the structural analysis, here it is derived in the same manner as restoring stiffness due to reasons of their relationship.

Variation of strain energy written in the index notation reads

$$\delta W = \iiint_{V} \sigma_{kl} \delta \varepsilon_{kl} \mathrm{d}V, \tag{25}$$

where σ_{kl} and ε_{kl} are the stress and strain tensors, respectively. The former is a function of the latter

$$\sigma_{kl} = \lambda \delta_{kl} \varepsilon_{mm} + 2\mu \varepsilon_{kl}, \tag{26}$$

where λ and μ are the Lamé constants, and δ_{kl} is the Kronecker symbol [15]. Strain tensor can be expressed with displacements

$$\varepsilon_{kl} = \varepsilon_{kl}^{0} + \varepsilon_{kl}^{*}, \tag{27}$$

where ε_{kl}^{0} and ε_{kl}^{*} are linear and non-linear terms

$$\varepsilon_{kl}^{0} = \frac{1}{2} \left(H_{k,l} + H_{l,k} \right) \tag{28}$$

$$\varepsilon_{kl}^{*} = \frac{1}{2} H_{m,k} H_{m,l} \tag{29}$$

3.2 Conventional stiffness

Strain energy Eq. (25) can also be written in the matrix notation. The linear tensor Eq. (28) leads to the conventional stiffness, while non-linear one, Eq. (29), results with non-linear geometric stiffness used in large displacement and structural instability analyses [16]. Thus,

$$\delta W^{0} = \iiint_{V} \sigma^{T} \delta \varepsilon^{0} \mathrm{d}V, \tag{30}$$

where σ and ε^{0} are stress and strain vectors with six terms

$$\mathbf{\acute{o}} = \mathbf{D}\mathring{\mathbf{a}}^{0}, \quad \mathring{\mathbf{a}}^{0} = \Lambda \mathbf{H}, \quad \mathbf{H^{T}} = \left\langle H_x, H_y, H_z \right\rangle. \tag{31}$$

D and Λ are elasticity matrix and matrix differential operator, respectively. Substituting Eq. (31) into Eq. (30) yields

$$\delta W^{0} = \iiint_{V} \left(\Lambda \mathbf{H} \right)^{T} \mathbf{D} \left(\Lambda \delta \mathbf{H} \right) \mathrm{d}V. \tag{32}$$

Furthermore, the modal superposition method, Eqs. (14), is used

$$\mathbf{H} = \left\langle \mathbf{h}_{\mathrm{j}} \right\rangle \left\{ \xi_j \right\} = \mathbf{h}\xi, \tag{33}$$

where **h** and ξ are modal matrix and mode amplitude vector respectively. By substituting Eq. (31) into Eq. (30) one finds

$$\delta W^{0} = \xi^{T} \mathbf{k}_{0} \delta \xi, \tag{34}$$

where

$$\mathbf{k}_{0} = \iiint_{V} \mathbf{B}^{T} \mathbf{D} \mathbf{B} \mathrm{d}V, \quad \mathbf{B} = \Lambda \mathbf{h} \tag{35}$$

are conventional stiffness matrix and strain-displacement transformation matrix respectively [17].

Structural problems are ordinarily solved by the finite element method. In that case modal matrix **h** represents matrix of shape (interpolation) functions. The above formulation is given for solids, but it can be easily adopted for thin-walled structural elements as constitutive parts of marine structures.

3.3 Geometric stiffness

For linear hydroelastic analysis of marine structures linearized geometric stiffness is sufficient. Therefore, constant stress is taken into account. Thus, after inserting Eq.(29) for non-linear part of strain tensor into (25), the following expression is obtained:

$$\delta W^{G} = \frac{1}{2} \iiint_{V} \sigma_{kl} \left[\delta H_{m,k} H_{m,l} + H_{m,k} \delta H_{m,l} \right] \mathrm{d}V. \tag{36}$$

The modal superposition terms Eq. (14) lead to the modal equation

$$\delta W_i^{G} = \sum_{j=1}^{N} k_{ij}^{G} \xi_j \delta \xi_i, \tag{37}$$

where

$$k_{ij}^{G} = \iiint_{V} \sigma_{kl} h_{m,k}^{i} h_{m,l}^{j} \mathrm{d}V \tag{38}$$

is geometric stiffness matrix.

Expression (38) is derived for solids. However, it can be also used for thin-walled marine structures. Thus, Eq. (38) applied to the plate finite element in the local coordinate system takes the well-known form [18, 19, 20]

$$k_{ij}^{G} = \iiint_{V} \left\langle \frac{\partial w^{i}}{\partial x}, \frac{\partial w^{i}}{\partial y} \right\rangle \begin{bmatrix} \sigma_{xx} & \sigma_{xy} \\ \sigma_{yx} & \sigma_{yy} \end{bmatrix} \begin{Bmatrix} \frac{\partial w^{j}}{\partial x} \\ \frac{\partial w^{j}}{\partial y} \end{Bmatrix} \mathrm{d}V, \qquad (39)$$

where w_i are deflection shape-functions, while σ_{xx}, σ_{yy}, and $\sigma_{xy} = \sigma_{yx}$ are the membrane stress components.

4 Unified geometric and restoring stiffness

In structural analysis of marine structures, conventional stiffness, $\mathbf{K}^0$, geometric stiffness, $\mathbf{K}^G$, and restoring stiffness, $\mathbf{C}$, are used. $\mathbf{K}^0$ is basic stiffness of any structure, while the application of $\mathbf{K}^G$ and $\mathbf{C}$ depends on analysis concerned as well as on the type of structure. $\mathbf{K}^G$ is used in the structural stability analysis and in the ultimate strength analysis of ship structure. Application of $\mathbf{C}$ is necessary in the ship hydroelastic analysis. For slender structures, like floating airports, TLP etc. both $\mathbf{K}^G$ and $\mathbf{C}$ have to be used. In that case union of $\mathbf{K}^G$ and $\mathbf{C}$ has to be determined since these matrices have some terms of equivalent sense due to the same external load, i.e. structure weight and hydrostatic pressure.

Hence, one can write

$$k_{ij}^{U} = k_{ij}^{G} \cup C_{ij} = k_{ij}^{G} + C_{ij} - k_{ij}^{GZ}, \qquad (40)$$

where

$$k_{ij}^{GZ} = k_{ij}^{G} \cap C_{ij} \qquad (41)$$

is the intersection of considered two sets related to vertical direction. If $\mathbf{C}_{ij}$ is used alone, then $\mathbf{K}^G$ terms related to axial and transverse directions are omitted.

The necessary stiffness k_{ij}^{GZ} can be determined by transforming Eq. (2e), Table 1, via integration by parts. In the standard procedure, $\int u\mathrm{d}v = uv - \int v\mathrm{d}u$, different combinations of u and v are possible. However, only the couple $u = \sigma_{kl} h_{m,l}^{j}$ and $\mathrm{d}v = h_{m,k}^{i}\mathrm{d}V$ lead to the transformations compatible to Eq. (4), in which displacement of the i mode occurs, in accordance with the conclusion 1 in Section 1. Thus, according to [9], one finds

$$k_{ij}^{G} = k_{ij}^{S} + k_{ij}^{V} + k_{ij}^{Vc}, \qquad (42)$$

where

$$k_{ij}^{S} = \iint_{S} \sigma_{kl} h_{m}^{i} h_{m,l}^{j} n_{k}\mathrm{d}S \qquad (43)$$

$$k_{ij}^{V} = -\iiint_{V} \sigma_{kl,k} h_{m}^{i} h_{m,l}^{j}\mathrm{d}V \qquad (44)$$

$$k_{ij}^{Vc} = -\iiint_{V} \sigma_{kl} h_{m}^{i} h_{m,lk}^{j}\mathrm{d}V. \qquad (45)$$

At the wetted surface, S, and within the structure volume, V, the following boundary and equilibrium conditions have to be satisfied [14], Figures 2 and 3, respectively

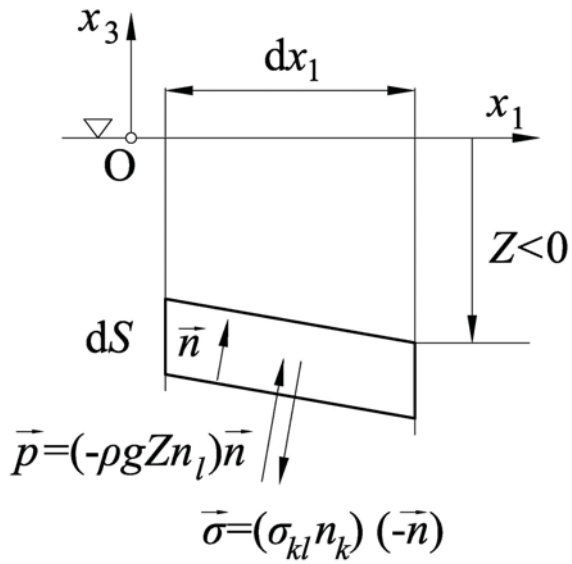

Figure 2 **Boundary condition for stresses expressed with hydrostatic pressure, $\vec{\sigma} = -\vec{p}$**
Slika 2 **Rubni uvjet za naprezanje izražen hidrostatskim tlakom, $\vec{\sigma} = -\vec{p}$**

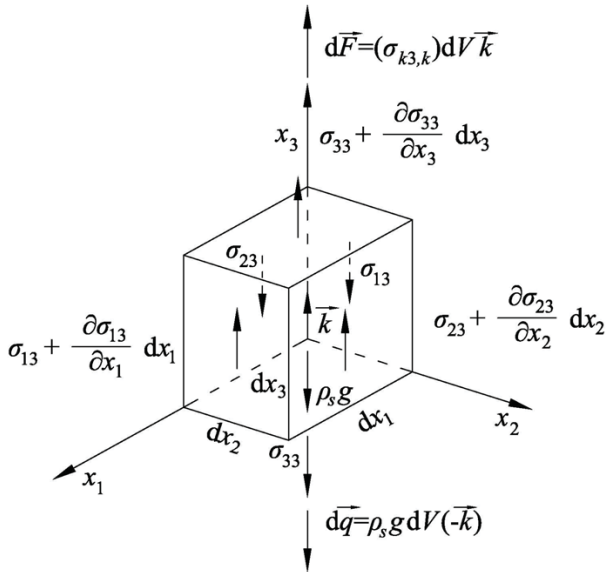

Figure 3 **Equilibrium condition of stresses and gravity load, $\mathrm{d}\vec{F} = -\mathrm{d}\vec{q}$**
Slika 3 **Uvjet ravnoteže naprezanja i gravitacijskog opterećenja, $\mathrm{d}\vec{F} = -\mathrm{d}\vec{q}$**

$$\sigma_{kl} n_{k} = -\rho g Z n_{l}, \quad \sigma_{k3,k} = \rho_{S} g, \qquad (46a, b)$$

while $\sigma_{k1,k} = \sigma_{k2,k} = 0$. Substituting Eqs. (46a, b) into Eqs. (43) and (44) respectively, yields

$$k_{ij}^{SZ} = -\rho g \iint_{S} Z h_{k}^{i} h_{k,l}^{j} n_{l}\mathrm{d}S \qquad (47)$$

$$k_{ij}^{VZ} = -g \iiint_{V} \rho_{S} h_{k}^{i} h_{k,3}^{j}\mathrm{d}V. \qquad (48)$$

Hydrostatic pressure and structure weight are equilibrated external load, and they are included in restoring stiffness, C_{ij}. Terms k_{ij}^{SZ} and k_{ij}^{VZ} are equivalent parts of geometric stiffness determined via stresses as internal structural reaction to the imposed load. Hence, the intersection matrix, Eq. (41), is

$$k_{ij}^{GZ} = k_{ij}^{SZ} + k_{ij}^{VZ}. \tag{49}$$

Furthermore, the unified stiffness, Eq. (40), by employing the constitutive parts of C_{ij}, Eq. (4), and Eq. (49) for k_{ij}^{GZ}, reads

$$k_{ij}^{U} = k_{ij}^{G} + C_{ij} - k_{ij}^{GZ} = k_{ij}^{G} + C_{ij}^{p} + C_{ij}^{nh} + C_{ij}^{m} - k_{ij}^{SZ} - k_{ij}^{VZ}. \tag{50}$$

Terms C_{ij}, Eq. (4d), and k_{ij}^{VZ}, Eq. (48), in (50) have the same factors and are condensed to one expression

$$C_{ij}^{m} - k_{ij}^{VZ} = g\iiint_{V} \rho_s h_k^i \left(h_{3,k}^j + h_{k,3}^j\right) \mathrm{d}V. \tag{51}$$

Table 2 **Unified geometric and restoring stiffness**
Tablica 2 **Objedinjena geometrijska i povratna krutost**

Transfer of	Notation	k_{ij}^{U}, Eq. (50) i.e. (52)		Contribution from
Eq. (4a)	C_{ij}^{p}	$\rho g \iint_{S} h_k^i h_3^j n_k \mathrm{d}S$	(52a)	Pressure
Eq. (4b)	C_{ij}^{nh}	$\rho g \iint_{S} Z h_k^i h_{l,l}^j n_k \mathrm{d}S$	(52b)	Normal vector and mode
Eq. (48)	$-k_{ij}^{SZ}$	$\rho g \iint_{S} Z h_k^i h_{k,l}^j n_l \mathrm{d}S$	(52c)	Boundary stress (elastic body)
Eq. (52)	$C_{ij}^{m} - k_{ij}^{VZ}$	$g\iiint_{V} \rho_s h_k^i \left(h_{3,k}^j + h_{k,3}^j\right) \mathrm{d}V$	(52d)	Gravity load and stress
Eq. (2e)	k_{ij}^{G}	$\iiint_{V} \sigma_{kl} h_{m,k}^i h_{m,l}^j \mathrm{d}V$	(52e)	Geometric stiffness

The unified stiffness, Eq. (50), is shown in the expanded form in Table 2, numbered as Eq. (52). The particular terms are transferred from the known and derived formulas, as it is indicated in the first column of the table. Comparing Eq. (53) with Eq. (2) in Table 1, it is obvious that the former has one term more than the latter, i.e. $C_{ij}^{m} - k_{ij}^{VZ}$, and terms k_{ij}^{SZ} and k_{ij}^{S0} are different. In the case of rigid body modes, the rotation angles are mutually dependent, i.e. $h_{3,k}^j = -h_{k,3}^j$, $k = 1,2$, and the spherical strain $h_{3,3}^j = 0$, so that term $C_{ij}^{m} - k_{ij}^{VZ}$, Eq. (53d), is reduced to the elastic modes.

Eq. (53c) can be written in the following form

$$-k_{ij}^{SZ} = \left(-k_{ij}^{SZ} + k_{ij}^{S0}\right) - k_{ij}^{S0} \tag{53}$$

where, by employing Eq. (2c) for k_{ij}^{S0}, yields

$$-k_{ij}^{SZ} + k_{ij}^{S0} = \rho g \iint_{S} Z h_k^i \left(h_{k,l}^j + h_{l,k}^j\right) n_l \mathrm{d}S. \tag{54}$$

If the structure mass is condensed in the wetted shell of the thickness proportional to $Z \le 0$ and $n_3 \ge 0$, i.e. $t = -\dfrac{\rho}{\rho_s} Z n_3$, the volume integral (52) can be transformed into the surface integral

$$C_{ij}^{m} - k_{ij}^{VZ} = -\rho g \iint_{S} Z h_k^i \left(h_{3,k}^j + h_{k,3}^j\right) n_3 \mathrm{d}S. \tag{55}$$

It is obvious that the dominant term for $l = 3$ in (54) is cancelled with (55). Hence, one can expect that in the general case sum of terms (51) and (54) represents a small difference of two large quantities, and therefore can be neglected in the unified restoring and geometric stiffness, Eq. (52). In that way the simplified unified stiffness is reduced to the so called complete restoring stiffness, Eq. (2).

The unified geometric and restoring stiffness, Eq. (52), is derived in a transparent way by the set theory approach. On the contrary, Eq. (2) is obtained by employing an advanced and quite different procedure based on a consistent linearization of the external hydrostatic pressure and the internal structural stresses [9]. Actually, derivation of Eq. (2) and Eq. (52) started from the opposite sides. The relations used in transformation of Eq. (2), [9, 14], are employed in derivation of Eq. (52). Since the simplified unified stiffness is equal to the complete restoring stiffness, the circle is closed, Eq. (2). Application of Eq. (2) is preferable due to less number of constitutive terms and symmetry.

Based on the above facts, transformation and specialization of Eq. (2) for rigid body motion is a reverse and inadequate step from the unified stiffness point of view [14]. It disputes exactness of Eq. (4) for elastic modes. However, Eq. (4) is derived for ship structures in a direct and transparent way based on the work of external forces, without making the distinction between rigid body and elastic modes.

5 Numerical procedure for hydroelastic analysis

Mathematical hydroelastic model comprises structural, hydrostatic and hydrodynamic one [4]. Here, the investigation is focused on restoring stiffness so structural model is not treated in detail, while the hydrodynamic model is not considered at all. It is shown that the gravity stiffness is the part of the geometric stiffness related to vertical direction. In ship hydroelastic analysis it is sufficient to take gravity stiffness into account, while for slender structures, as floating airports and tension leg platforms, the unified geometric and restoring stiffness has to be used [5].

Since the static configuration is referent one for dynamic response and vibrations, the hydroelastic analysis for slender structures should be consisted of the following steps:

1. 3D FEM strength analysis in still water, $\mathbf{K}_0\boldsymbol{\delta}_0 = \mathbf{F}_0$, where load consists of the equilibrated weight and buoyancy.
2. Calculation of geometric stiffness $\mathbf{K}_G$ based on the known static stress distribution from the previous step.
3. Correction of nodal coordinates in 3D FEM model due to statical displacements (if significant), $\mathbf{x} = \mathbf{x}_0 + \boldsymbol{\delta}_0$ and consequently definition of new wetted surface.
4. Dry natural vibrations analysis of the statically equilibrated FEM model as the referent state, by one of the eigenvalue equations:
$$\left(\mathbf{K}_0 - \Omega^2\mathbf{M}\right)\boldsymbol{\delta} = \mathbf{0}, \quad \left(\mathbf{K}_0 + \mathbf{K}_G - \Omega^2\mathbf{M}\right)\boldsymbol{\delta} = \mathbf{0}. \tag{56a, b}$$
5. Calculation of modal matrices $\mathbf{k}_0$, $\mathbf{m}$ and $\mathbf{k}^{\mathrm{U}}$; or $\mathbf{k}_{0G} = \mathbf{k}_0 + \mathbf{k}_G$, $\mathbf{m}$ and $\mathbf{C}$, respectively.
6. Calculation of hydrodynamic coefficients $\mathbf{B}(\omega)$ and $\mathbf{A}(\omega)$, and wave load $\mathbf{F}_w$.
7. Solution of the equation for fluid-structure interaction:
$$\mathbf{k}_{0GC}\boldsymbol{\delta} + \left(\mathbf{b} + \mathbf{B}(\omega)\right)\dot{\boldsymbol{\delta}} + \left(\mathbf{m} + \mathbf{A}(\omega)\right)\ddot{\boldsymbol{\delta}} = \mathbf{F}_w, \tag{57}$$

where, according to (56a, b), $\mathbf{k}_{0GC} = \mathbf{k}_0 + \mathbf{k}^U$ and $\mathbf{k}_{0GC} = \mathbf{k}_{0G} + \mathbf{C}^*$ respectively.

6 Pontoon unified geometric and restoring stiffness

6.1 General

Application of previously presented theory is illustrated in the case of a prismatic pontoon. The problem is solved analytically according to Eq. (2), in order to get better insight into physical background through constitution of governing equations and to prove consistency of the theory.

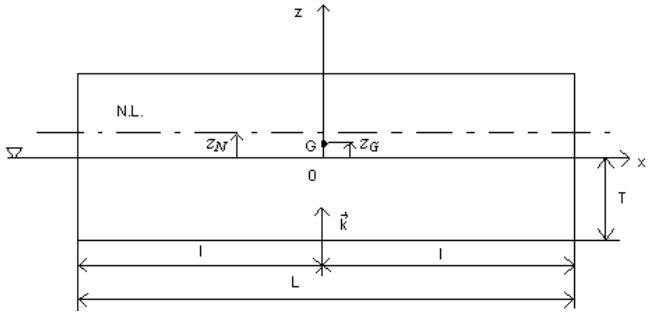

Figure 4 **Pontoon main particulars**
Slika 4 **Globalne značajke pontona**

The main pontoon particulars are shown in Figure 4. The modal displacement vector due to vertical deflection *w* reads

$$\mathbf{H} = -\frac{\mathrm{d}w}{\mathrm{d}x}\left(Z - z_N\right)\mathbf{i} + w\mathbf{k}, \tag{58}$$

where z_N is the vertical position of neutral line (centroid) of pontoon cross-section. Thus,

$$h_1 = h_x = -\left(Z - z_N\right)\frac{\mathrm{d}w}{\mathrm{d}x}, \quad h_2 = h_y = 0, \quad h_3 = h_z = w. \tag{59}$$

In the considered case $h_{x,z} = -h_{z,x} = -\dfrac{\mathrm{d}w}{\mathrm{d}x}$ and $h_{z,z} = 0$, and consequently $C_{ij}^m - k_{ij}^{VZ} = 0$, Eq. (51). Also, at the bottom and heads $h_{x,x}n_1 = 0$ and $h_{z,z}n_3 = 0$, that gives $-k_{ij}^{SZ} + k_{ij}^{S0} = 0$, Eq. (54). Based on the above conclusion Eq. (2) is used for determining the unified restoring and geometric stiffness.

6.2 Restoring stiffness, Eqs. (2a), (2b), (2c)

Pontoon bottom
General data: $\mathrm{d}S = B\mathrm{d}x, \quad Z = -T, \quad n_3 = n_z = \left|\mathbf{k}\right|$

$$C_{ij}^p = \rho g B\int_{-l}^{l} w_i w_j \mathrm{d}x \tag{60}$$

$$C_{ij}^{nh} = \rho g B\int_{-l}^{l} Z h_z^i h_{x,x}^j n_z \mathrm{d}x = F_p\int_{-l}^{l}\frac{\mathrm{d}w_i}{\mathrm{d}x}\frac{\mathrm{d}w_j}{\mathrm{d}x}\mathrm{d}x - F_p\left(w_i\frac{\mathrm{d}w_j}{\mathrm{d}x}\right)_{-l}^{l} \tag{61}$$

$$-k_{ij}^{S0} = -\rho g B\int_{-l}^{l} Z h_x^i h_{z,x}^j n_z \mathrm{d}x = F_p\int_{-l}^{l}\frac{\mathrm{d}w_i}{\mathrm{d}x}\frac{\mathrm{d}w_j}{\mathrm{d}x}\mathrm{d}x, \tag{62}$$

where

$$F_p = \rho g B T\left(T + z_N\right). \tag{63}$$

Pontoon heads
General data: $n_1 = n_x = -\left|\mathbf{i}\right|$ for front head,
$n_1 = n_x = \left|\mathbf{i}\right|$ for aft head
$Z_0 = 0, \quad Z_{bottom} = -T, \quad \mathrm{d}S = B\mathrm{d}z$

$$C_{ij}^p = \rho g B\int_{-T}^{0}\left(h_x^i h_z^j n_x\right)_{-l}^{l}\mathrm{d}Z = -F_H\left(\frac{\mathrm{d}w_i}{\mathrm{d}x}w_j\right)_{-l}^{l} \tag{64}$$

$$C_{ij}^{nh} = \rho g B\int_{-T}^{0}\left(h_x^i h_{x,x}^j n_x\right)_{-l}^{l}\mathrm{d}Z = B_{nh}\left(\frac{\mathrm{d}w_i}{\mathrm{d}x}\frac{\mathrm{d}^2 w_j}{\mathrm{d}x^2}\right)_{-l}^{l} \tag{65}$$

$$\begin{aligned} -k_{ij}^{S0} &= -\rho g B\int_{-T}^{0} Z\left(h_x^i h_{x,x}^j n_x + h_z^i h_{x,z}^j n_x\right)_{-l}^{l}\mathrm{d}Z = \\ &= -B_{nh}\left(\frac{\mathrm{d}w_i}{\mathrm{d}x}\frac{\mathrm{d}^2 w_j}{\mathrm{d}x^2}\right)_{-l}^{l} + N_0\left(w_i\frac{\mathrm{d}w_j}{\mathrm{d}x}\right)_{-l}^{l}, \end{aligned} \tag{66}$$

where

$$F_H = \rho g B T\left(\frac{T}{2} + z_N\right), \quad N_0 = \frac{1}{2}\rho g B T^2 \tag{67}$$

$$B_{nh} = \frac{1}{2}\rho g B T^2\left(\frac{T^2}{2} + \frac{4}{3}T z_N + z_N^2\right). \tag{68}$$

6.3 Geometric stiffness, Eq. (2e)

General data: $\mathrm{d}V = \mathrm{d}A\mathrm{d}x$

$$\begin{aligned} k_{ij}^G &= \int_{-l}^{l}\iint_A\left[\sigma_{xx}\left(h_{x,x}^i h_{x,x}^j + h_{z,x}^i h_{z,x}^j\right) + \sigma_{zz}h_{x,z}^i h_{x,z}^j\right]\mathrm{d}A\mathrm{d}x = \\ &= \int_{-l}^{l}\iint_A\left\{\sigma_{xx}\left[\left(Z - z_N\right)\frac{\mathrm{d}^2 w_i}{\mathrm{d}x^2}\frac{\mathrm{d}^2 w_j}{\mathrm{d}x^2} + \frac{\mathrm{d}w_i}{\mathrm{d}x}\frac{\mathrm{d}w_j}{\mathrm{d}x}\right] + \sigma_{zz}h_{x,z}^i h_{x,z}^j\right\}\mathrm{d}A\mathrm{d}x. \end{aligned} \tag{69}$$

The first term in Eq. (69) with curvatures is negligible compared to the others. The second term is related to the axial direction, where σ_{xx} is equal to the head hydrostatic pressure. Thus, one finds the compression axial force, Figure 5,

Figure 5 **Static boundary load**
Slika 5 **Statičko rubno opterećenje**

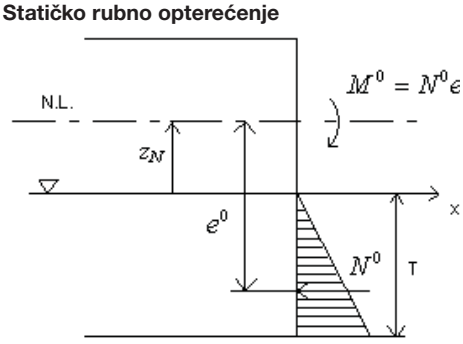

$$\iint_A \sigma_{xx}\mathrm{d}A = \rho g B \int_{-T}^{0} Z\mathrm{d}Z = -N_0 \tag{70}$$

that gives stiffness of the axial direction

$$k_{ij}^{GX} = -N_0 \int_{-l}^{l} \frac{\mathrm{d}w_i}{\mathrm{d}x}\frac{\mathrm{d}w_j}{\mathrm{d}x}\mathrm{d}x. \tag{71}$$

In order to determine stiffness of the vertical direction, it is necessary to apply integration by parts for the third term in Eq. (69), $(u = \sigma_{zz} h_{x,z}^{j},\ \ \mathrm{d}v = h_{x,z}^{i}\mathrm{d}z)$. Actually, this is the reverse procedure of that used in formulation of unified restoring stiffness, Eq. (43):

$$k_{ij}^{GZ} = B\int_{-l}^{l}\left(\sigma_{zz} h_x^i h_{x,z}^j\right)_{z=-T}^{z=0}\mathrm{d}x - \int_{-l}^{l}\iint_A \left(\sigma_{zz,z} h_x^i h_{x,z}^j\right)\mathrm{d}A\mathrm{d}x. \tag{72}$$

The first term in Eq. (72) is put in order by taking $\sigma_{zz}(0) = 0$ and $\sigma_{zz}(-T) = -\rho g T$ into account. The second term, with $\sigma_{zz,z} = g\rho_S$, occurs in the form

$$-g\int_{-l}^{l}\iint_A \rho_S\left(Z - z_N\right)\frac{\mathrm{d}w_i}{\mathrm{d}x}\frac{\mathrm{d}w_j}{\mathrm{d}x}\mathrm{d}A\mathrm{d}x,$$

which represents static moment of the mass distribution per pontoon cross-section with respect to the centroid, z_N. Since, $\iint_A \rho_S \mathrm{d}A = m = \rho BT$ for Eq. (72) one can write

$$k_{ij}^{GZ} = -\left(F_p + F_g\right)\int_{-l}^{l}\frac{\mathrm{d}w_i}{\mathrm{d}x}\frac{\mathrm{d}w_j}{\mathrm{d}x}\mathrm{d}x, \tag{73}$$

where

$$F_g = \rho g B T\left(z_G - z_N\right) \tag{74}$$

and z_G is the centre of gravity coordinate, Figure 2.

6.4 Unified stiffness

After specifying the constitutive parts, it is possible to assemble the unified stiffness. In that process some terms are cancelled: $-k_{ij}^{S0}$ of the bottom with the first term of k_{ij}^{GZ}; C_{ij}^{nh} with the first term of $-k_{ij}^{S0}$ both for the heads. Thus, the unified stiffness is reduced to

$$k_{ij}^{U} = \rho g B I_{ij}^{(0)} + \left(F_p - F_g - N_0\right)I_{ij}^{(1)} + \left(N_0 - F_p\right)\left(w_i\varphi_j\right)_{-l}^{l} - \\ -F_H\left(\varphi_i w_j\right)_{-l}^{l}, \tag{75}$$

where $\varphi = \mathrm{d}w/\mathrm{d}x$ and

$$I_{ij}^{(0)} = \int_{-l}^{l} w_i w_j \mathrm{d}x, \quad I_{ij}^{(1)} = \int_{-l}^{l}\frac{\mathrm{d}w_i}{\mathrm{d}x}\frac{\mathrm{d}w_j}{\mathrm{d}x}\mathrm{d}x. \tag{76}$$

If relation $F_p - N_0 = F_H$ is used, Eq. (75) can be presented in the recognizable symmetric form

$$k_{ij}^{U} = \rho g B I_{ij}^{(0)} + \left(F_H - F_g\right)I_{ij}^{(1)} - F_H\left[\left(w_i\varphi_j\right)_{-l}^{l} + \left(\varphi_i w_j\right)_{-l}^{l}\right]. \tag{77}$$

Consistency of the above formulae can be checked in the case of rigid body modes. The heave natural modes, $w_0 = 1$, gives $k_{00}^{U} = \rho g L B$, i.e. the stiffness value equal to that in the ship hydrostatics [21]. The pitch natural mode is $w_1 = x$, $\varphi_1 = 1$, $-l \le x \le l$, so that $I_{11}^{(0)} = \frac{L^3}{12}$ and $I_{11}^{(1)} = L$. That gives

$$k_{11}^{U} = -\rho g L B T\left(\frac{T}{2} + z_G\right) + \rho g\frac{BL^3}{12}. \tag{78}$$

Since $V = LBT$ is the displaced volume and $\frac{BL^3}{12} = I_{WLY}$ is the longitudinal moment of inertia of the waterplane area, the unified stiffness takes the form

$$k_{11}^{U} = \rho g\left[I_{WLY} - V\left(\frac{T}{2} + z_G\right)\right] \tag{79}$$

It is identical to the hydrostatic expression, because the coordinate of the centre of buoyancy takes value $z_B = -\frac{T}{2}$, [21].

7 Pontoon vibrations

The modal superposition method utilizing dry modes is commonly used to solve hydroelastic problems. In the considered case of homogenous pontoon, the differential equation of vertical dry natural vibrations reads

$$\frac{\mathrm{d}^4 w}{\mathrm{d}x^4} - \Omega^2\frac{m}{EI}w = 0 \tag{80}$$

with the following well-known modes for the case of free beam [22].

Symmetric modes

$$w_n = \frac{1}{2}\left[\frac{\mathrm{ch}\beta_n x}{\mathrm{ch}\beta_n l} + \frac{\cos\beta_n x}{\cos\beta_n l}\right], \quad n = 0,2,4\ldots \\ \beta_0 l = 0, \quad \beta_2 l = 2.365, \quad \beta_4 l = 5.497. \tag{81}$$

Anti-symmetric modes

$$w_n = \frac{1}{2}\left[\frac{\mathrm{sh}\beta_n x}{\mathrm{sh}\beta_n l} + \frac{\sin\beta_n x}{\sin\beta_n l}\right], \quad n = 1,3,5\ldots \\ \beta_1 l = 0, \quad \beta_3 l = 3.925, \quad \beta_5 l = 7.068 \\ \lim_{n\to\infty}\beta_n l = \frac{2n-1}{4}\pi \tag{82}$$

Natural frequencies in air

$$\Omega_n = \frac{\left(\beta_n l\right)^2}{l^2}\sqrt{\frac{EI}{m}}, \quad n = 0,1,2\ldots \tag{83}$$

By assuming forced response in the series of the natural modes

$$w = \sum_{j=0}^{N}\xi_j w_j \tag{84}$$

and employing the variational method, the following system of the algebraic equations is constituted

$$\sum_{j=0}^{N}\left[EI\cdot I_{ij}^{(2)}+\left(F_p-F_g-N_0\right)I_{ij}^{(1)}+\left(\rho gB-\omega^2 m_t\right)I_{ij}^{(0)}+\left(N_0-F_p\right)\left(w_i\varphi_j\right)_{-l}^{l}-F_H\left(\varphi_i w_j\right)_{-l}^{l}\right]\xi_i = \int_{-l}^{l} q_x w_i \mathrm{d}x,\quad i=0,1,2\ldots N, \tag{85}$$

where ω is the wave frequency and

$$I_{ij}^{(2)}=\int_{-l}^{l}\frac{\mathrm{d}^2 w_i}{\mathrm{d}x^2}\frac{\mathrm{d}^2 w_j}{\mathrm{d}x^2}\mathrm{d}x. \tag{86}$$

It is necessary to point out that $I_{ij}^{(0)}=I_{ij}^{(2)}=0$ if $i\neq j$ due to orthogonality of dry modes.

Eq. (83) can be presented in the matrix notation

$$\left(\mathbf{k}_0+\mathbf{k}^{\mathrm{U}}-\omega^2\mathbf{m}\right)\xi=\mathbf{F}, \tag{87}$$

where $\mathbf{k}_0 = E/\mathbf{I}^{(2)}$ and $\mathbf{m} = m_t\mathbf{I}^{(0)}$ are ordinary diagonal bending stiffness and mass matrices respectively, and $\mathbf{k}^{\mathrm{U}}$ is the unified geometric and restoring stiffness matrix, Eq. (2).

8 Beam finite element

In the finite element method the shape functions are used in the general formulation of the governing matrices instead of natural modes. For the ordinary two node beam finite element for flexural vibrations the Hermitian polynomials of the third order are used,

$$w_i=\left\langle a_{ik}\right\rangle\left\{\xi^k\right\};\quad i=1,2,3,4;\quad k=0,1,2,3, \tag{88}$$

where a_{ik} are the coefficients, $\xi=\dfrac{x}{L}$ is the non-dimensional coordinate and L is the element length. Symbols $\langle\ldots\rangle$ and $\{\ldots\}$ denote row and column vectors respectively. Matrix of the shape function coefficients reads

$$\mathbf{a}=\begin{bmatrix}1&0&-3&2\\0&L&-2L&L\\0&0&3&2\\0&0&-L&L\end{bmatrix} \tag{89}$$

Thus, for the integral matrices in Eqs. (76) and (86) one finds

$$\mathbf{I}^{(0)}=\frac{L}{420}\begin{bmatrix}156&22L&54&-13L\\&4L^2&13L&-3L^2\\&&156&-22L\\Sym.&&&4L^2\end{bmatrix} \tag{90}$$

$$\mathbf{I}^{(1)}=\frac{1}{30L}\begin{bmatrix}36&3L&-36&3L\\&4L^2&-3L&-L^2\\&&36&-3L\\Sym.&&&4L^2\end{bmatrix} \tag{91}$$

$$\mathbf{I}^{(2)}=\frac{2}{L^3}\begin{bmatrix}6&3L&-6&3L\\&2L^2&-3L&L^2\\&&36&-3L\\Sym.&&&2L^2\end{bmatrix} \tag{92}$$

Boundary values of the shape functions that differ from zero are the following:

$$w_1(0)=1,\quad \varphi_2(0)=1,\quad w_3(L)=1,\quad \varphi_4(L)=1$$

therefore the boundary value matrix yields

$$\left[\left(w_i\varphi_j\right)_0^L\right]=\begin{bmatrix}0&-1&0&0\\0&0&0&0\\0&0&0&1\\0&0&0&0\end{bmatrix},\quad \left[\left(\varphi_i w_j\right)_0^L\right]=\left[\left(w_i\varphi_j\right)_0^L\right]^T. \tag{93}$$

It is obvious that the integral matrices are symmetric, as well as the couple of the boundary matrices. After the integral and boundary matrices are determined, the finite element stiffness and mass properties can be completed according to Eq. (85), where all parameters depend on the finite element cross-section.

Consistency of the derived finite element properties can be checked in case of the rigid body modes of self equilibrated element. The nodal displacement vector for heave reads

$$\mathbf{w}_0^T=\langle 1,0,1,0\rangle \tag{94}$$

that gives

$$\begin{aligned}&\mathbf{w}_0^T\mathbf{I}^{(0)}\mathbf{w}_0=L\\&\mathbf{w}_0^T\mathbf{I}^{(1)}\mathbf{w}_0=0\\&\mathbf{w}_0^T\mathbf{I}^{(2)}\mathbf{w}_0=0\\&\mathbf{w}_0^T\left[\left(w_i\varphi_j\right)_0^L\right]\mathbf{w}_0=0.\end{aligned} \tag{95}$$

Thus, according to Eq. (85) one finds the following values for the stiffness and mass coefficients:

$$k_{00}^0=0,\quad k_{00}^U=\rho gBL,\quad m_{00}=m_t L. \tag{96}$$

The pitch nodal vector reads

$$\mathbf{w}_1^T=\langle -l,1,l,1\rangle \tag{97}$$

that leads to

$$\begin{aligned}&\mathbf{w}_1^T\mathbf{I}^{(0)}\mathbf{w}_1=\frac{L^3}{12}\\&\mathbf{w}_1^T\mathbf{I}^{(1)}\mathbf{w}_1=L\\&\mathbf{w}_1^T\mathbf{I}^{(2)}\mathbf{w}_1=0\\&\mathbf{w}_1^T\left[\left(w_i\varphi_j\right)_0^L\right]\mathbf{w}_1=L.\end{aligned} \tag{98}$$

Finally, the pontoon stiffness and mass properties, Eq. (85), take the following form:

$$k_{11}^0=0,\quad k_{11}^U=\rho g\left[I_{WL}-V\left(\frac{T}{2}+z_G\right)\right],\quad m_{11}=m_t\frac{L^3}{12} \tag{99}$$

It is obvious that the heave and pitch restoring stiffness are equal to those from the ship hydrostatics [21].

9 Illustrative example

In order to analyze restoring stiffness, let us consider a quite flexible segmented barge consisting of 12 equal prismatic pontoons [11, 23]. The pontoons are connected by means of two steel bars somewhat above the deck level, as shown in Figure 6. Two configurations with bar profiles of 50 x 4 and 50 x 6 mm are used. The main barge particulars are the following:

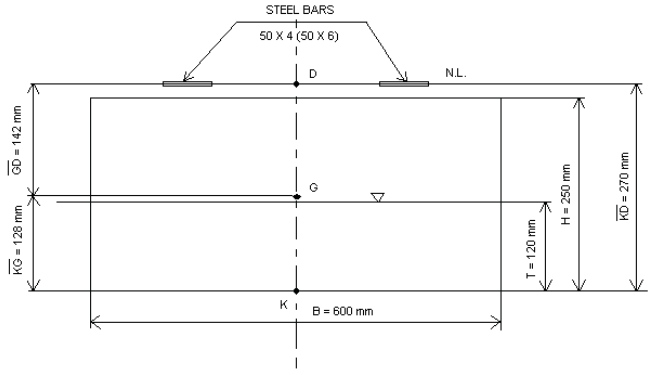

Figure 6 **Barge cross-section**
Slika 6 **Poprečni presjek barže**

Young's modulus of steel bars	$E = 2.0 \times 10^{11}$ N/m^2
Moment of inertia of cross-section	
Two bars 50x4 mm	$Iy = 5.33 \times 10^{-10}$ m^4
Two bars 50x6 mm	$Iy = 18.00 \times 10^{-10}$ m^4
Pontoon length	$l_p = 0.19$ m
Barge length (pontoons + clearances)	$L = 2.445$ m
Barge breadth	$B = 0.6$ m
Barge height	$H = 0.25$ m
Barge draught	$T = 0.12$ m
Vertical coordinate of gravity centre from waterline	$z_G = 0.008$ m
Vertical coordinate of neutral line from waterline	$z_N = 0.15$ m
Barge mass	$M = 176$ kg

Distributed mass $$m = \frac{M}{L} = 72 \quad \text{kg}$$

Distributed mass moment of inertia $$J_y \approx m\frac{H^2}{12} = 0.375 \quad \text{kgm}$$

In hydroelastic analysis the barge is treated as a monohull. The basic quantities occurring in the stiffness matrices take the following values:

$$\rho g B = 5.886 \times 10^3 \quad \text{N/m}^2$$
$$F_p = 0.1907 \times 10^3 \quad \text{N}$$
$$F_H = 0.1483 \times 10^3 \quad \text{N}$$
$$F_g = -0.100297 \times 10^3 \quad \text{N}$$
$$N_0 = 0.04238 \times 10^3 \quad \text{N.}$$

The integral and boundary matrices are specified in Appendix B. The geometric stiffness matrix, Eqs. (71) and (72), reads

$$\mathbf{k}^G = -\left(F_p + F_g + N_0\right)\mathbf{I}^{(1)} \tag{100}$$

However, its axial part $-N_0\mathbf{I}^{(1)}$ is neglected here since axial force is not used in ship longitudinal analysis as a part of geometric stiffness due to very small influence on response. On the other hand, term $-\left(F_p + F_g\right)\mathbf{I}^{(1)}$ is the part of ordinary restoring stiffness **C**, Eq. (4). Therefore, the pontoon vibrations are calculated with **C**, which is obtained from Eq. (75) by ignoring N_0

$$C_{ij} = \rho g B I_{ij}^{(0)} + \left(F_p - F_g\right) I_{ij}^{(1)} - F_p\left(w_i\varphi_j\right)_{-l}^{l} - F_H\left(\varphi_i w_j\right)_{-l}^{l}. \tag{101}$$

Table 3 **Modal restoring stiffness, analytical, C** [10^3]
Tablica 3 **Modalna povratna krutost, analitički, C** [10^3]

14.391	0.000	-0.725	0.000	-1.723	0.000
0.000	7.052	0.000	-1.222	0.000	-2.413
-0.564	0.000	3.781	0.000	-1.235	0.000
0.000	-0.974	0.000	4.670	0.000	-1.446
-1.341	0.000	-1.014	0.000	6.130	0.000
0.000	-1.899	0.000	-1.228	0.000	8.157

Table 4 **Modal restoring stiffness, numerical, C** [10^3]
Tablica 4 **Modalna povratna krutost, numerički, C** [10^3]

14.391	-0.036	-0.822	0.000	-1.848	0.000
-0.360	7.048	0.001	-1.343	0.005	-2.549
-0.660	0.001	3.829	0.000	-0.153	0.000
0.000	-1.090	0.000	4.840	0.273	-1.530
-1.460	0.004	-1.085	0.000	6.439	0.000
0.000	-2.025	0.000	-1.306	0.000	8.730

The restoring stiffness matrix determined analytically by Eq. (101) and analytical modes, Eqs. (81) and (82) is shown in Table 3 for the two rigid modes and two symmetric and anti-symmetric elastic modes. It is also calculated numerically according to the general formulae Eq. (4) and numerical natural modes, Table 4. Diagonal terms in Tables 3 and 4, which are predominant, agree quite well, especially the rigid body ones. Small differences between the terms of elastic modes and discrepancies of off-diagonal terms are mainly the result of small disagreement between numerically and analytically determined natural modes. The first two elastic vertical natural modes of the wetted surface, obtained by spreading the beam displacements *w* and d*w*/d*x*, Eq. (58), are shown in Figures 7 and 8.

For illustration purposes, the transfer functions of vertical bending moment in head sea for the both barge configurations are shown in Figure 9. They are calculated numerically by program DYANA [24], while the hydrodynamic coefficients (added mass and damping) are determined by program HYDROSTAR [25]. Ten elastic natural modes are taken into account, as well as the mass moment of inertia, J_y, via corresponding kinetic energy

$$E_{ij} = -\omega^2 J_y I_{ij}^{(1)} \tag{102}$$

added to Eq. (85), which changes the shape of higher natural modes and level of response and gives more realistic results.

The basic condition for the consistent restoring stiffness is convergence of transfer function to zero as wave frequency approaches zero value. This condition is satisfied for the elastic, as well as for the rigid body response. Large differences between

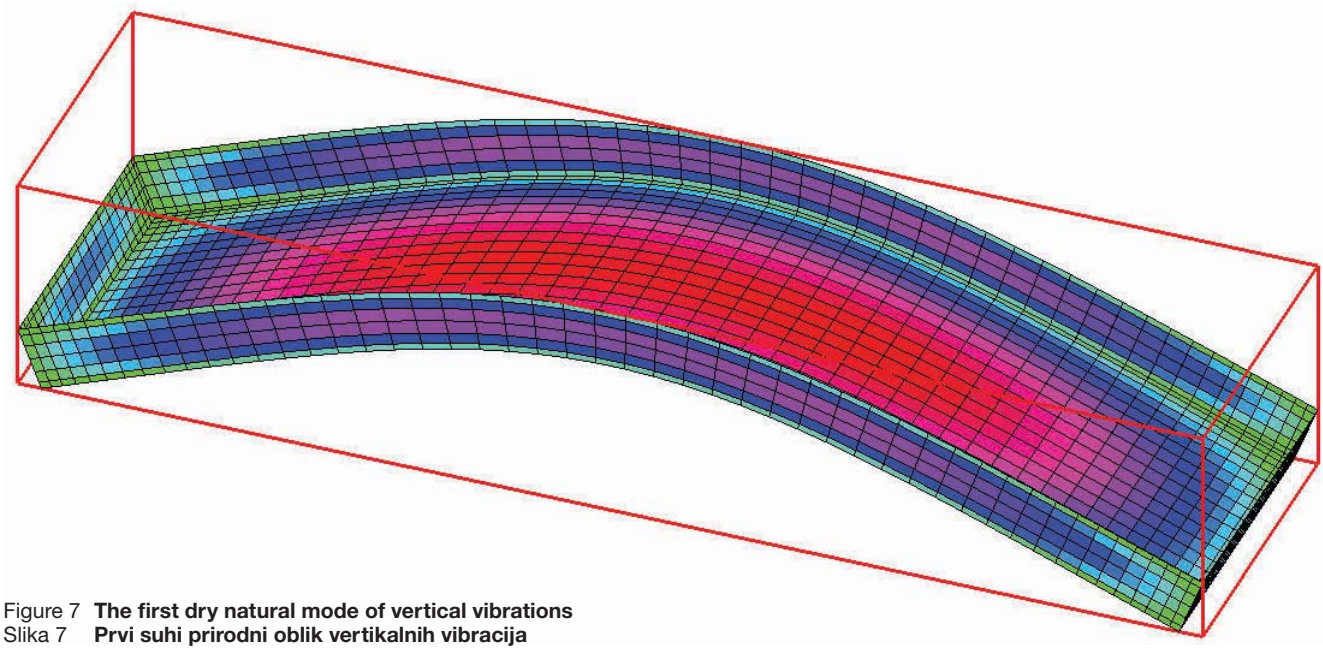

Figure 7 **The first dry natural mode of vertical vibrations**
Slika 7 **Prvi suhi prirodni oblik vertikalnih vibracija**

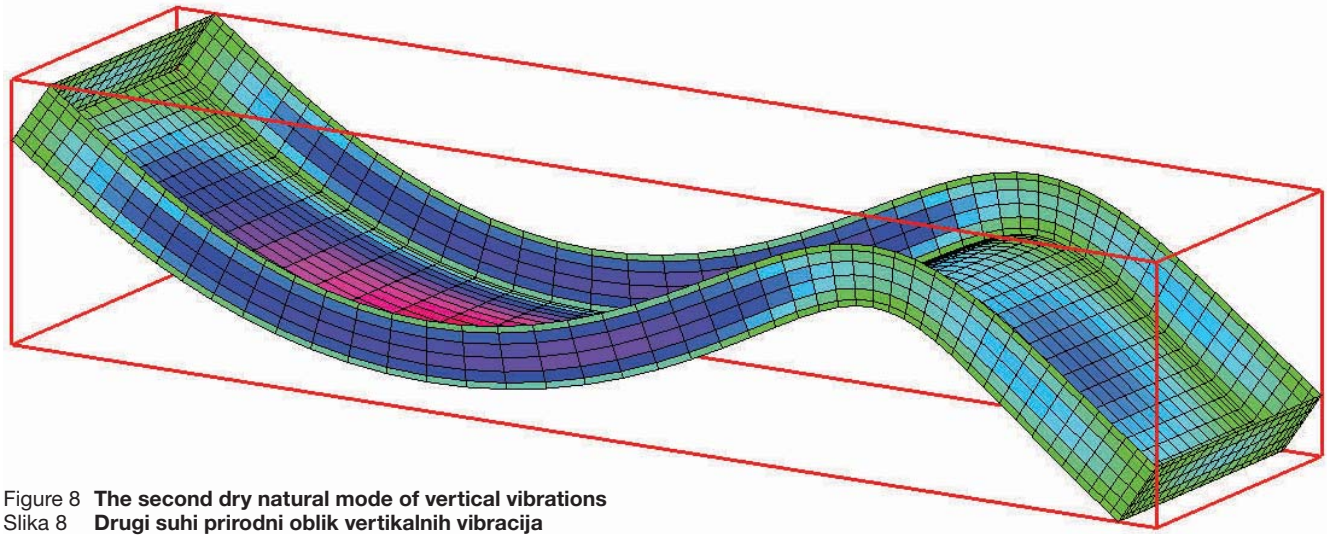

Figure 8 **The second dry natural mode of vertical vibrations**
Slika 8 **Drugi suhi prirodni oblik vertikalnih vibracija**

Figure 9 **Transfer function of vertical bending moment at mid-ship**
Slika 9 **Prijenosna funkcija vertikalnog momenta savijanja na sredini barže**

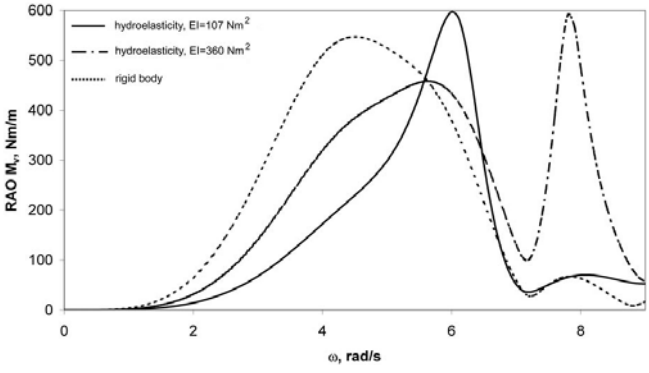

these responses at the very beginning of the wave frequency, ω, are the result of very small bending stiffness. Tendency of elastic response to follow the rigid body one for higher stiffness is obvious. The resonant peak for the softer and stiffer barge configuration occurs at $\omega = 6$ and 8 rad/s, respectively.

A series of model tests on the segmented barge has been conducted in BGO – First (Toulon – France), in order to validate numerical procedure, Figure 10 [23]. Numerical and measured transfer functions of the first mode flexural deformation for the both barge configurations are shown in Figures 11 and 12. Flexural deformation is defined as the difference between pitch angles of the first and last pontoon. These pitch angles are quite sensitive parameters to describe the barge flexural deformation, and that could be one of the reasons for disagreement between the calculated and measured responses which manifests with different peak values and corresponding resonant frequencies. Another

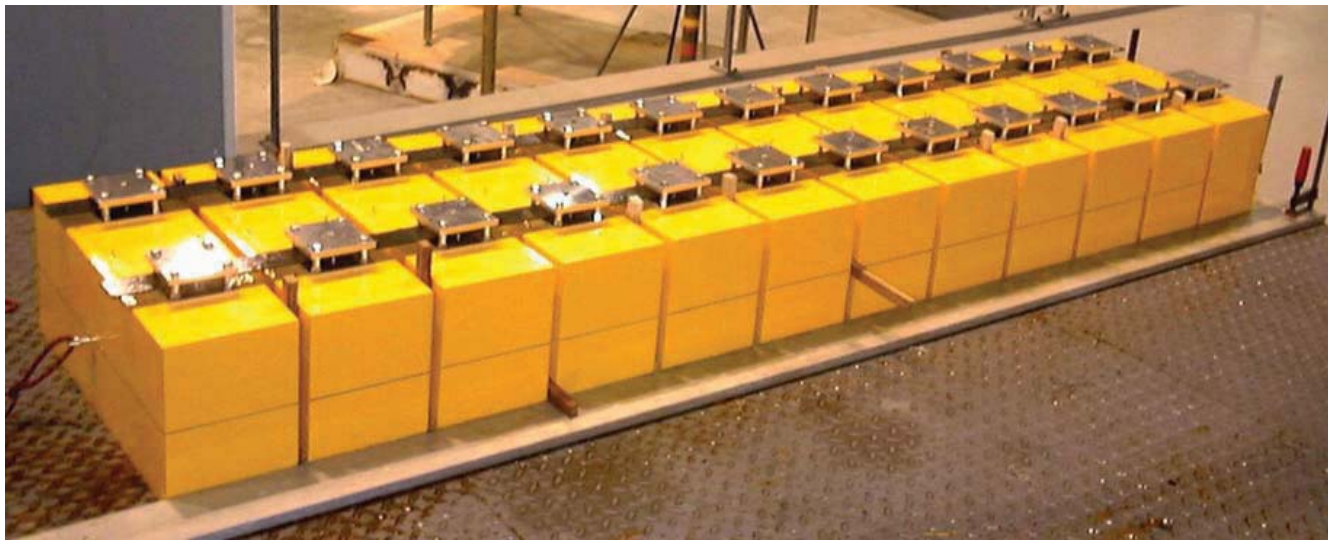

Figure 10 **Segmented barge**
Slika 10 **Segmentna barža**

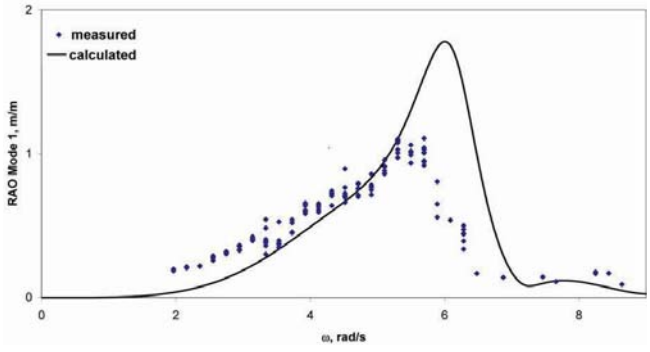

Figure 11 **Transfer function of amplitude of the 1st elastic mode, *EI* = 107 Nm², restoring stiffness C**
Slika 11 **Prijenosna funkcija amplitude prvog elastičnog oblika, *EI* = 107 Nm², povratna krutost C**

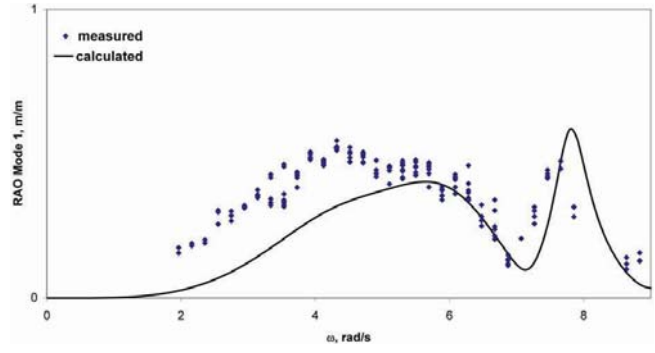

Figure 12 **Transfer function of amplitude of the 1st elastic mode, *EI* = 306 Nm², restoring stiffness C**
Slika 12 **Prijenosna funkcija amplitude prvog elastičnog oblika, *EI* = 306 Nm², povratna krutost C**

reason of discrepancies could be the amount of the assumed damping [3]. If Figures 11 and 12 are compared, it is obvious that the resonant peak in the former is split into two peaks in the latter due to increased flexural stiffness. Correlation of the other transfer functions is much better than those shown in Figures 11 and 12 [3, 11, 24].

Table 5 **Unified stiffness matrix, analytical, k^U [10^3]**
Tablica 5 **Objedinjena matrica krutosti, analitički, k^U [10^3]**

14.391	0.000	-0.564	0.000	-1.341	0.000
0.000	7.052	0.000	-0.974	0.000	-1.899
-0.564	0.000	3.728	0.000	-1.006	0.000
0.000	-0.974	0.000	4.470	0.000	-1.205
-1.341	0.000	-1.006	0.000	5.700	0.000
0.000	-1.899	0.000	-1.205	0.000	7.412

If the unified geometric and restoring stiffness is taken into account according to Eq. (77), its symmetric form is noticeable, Table 5. The forced response is determined for the first barge configuration, i.e. EI = 107 Nm² and excluding mass rotation, Eq. (102). Deflection is described with 8 natural modes. The transfer function of vertical bending moment is shown in Figure 13 and compared with that determined with ordinary restoring stiffness **C**, Table 4. Some differences are noticeable at resonant frequency $\omega = 6$ rad/s.

It is necessary to point out that the transfer function of bending moment determined with the unified stiffness does not converge to zero as the wave frequency approaches zero value, Figure 14. That negligible residuum is possibly result of axial force N_0 acting far from the neutral axis that should be further investigated, Fig. 6.

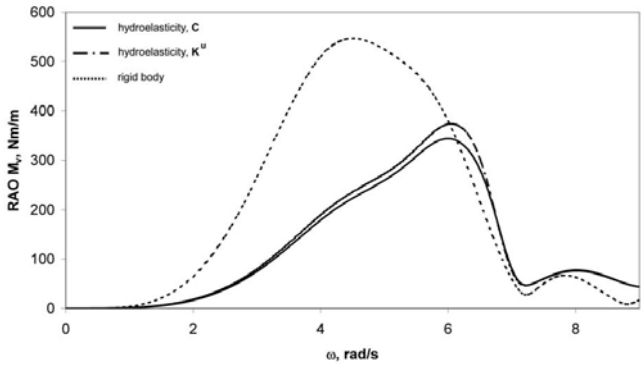

Figure 13 **Transfer function of vertical bending moment**
Slika 13 **Prijenosna funkcija vertikalnog momenta savijanja**

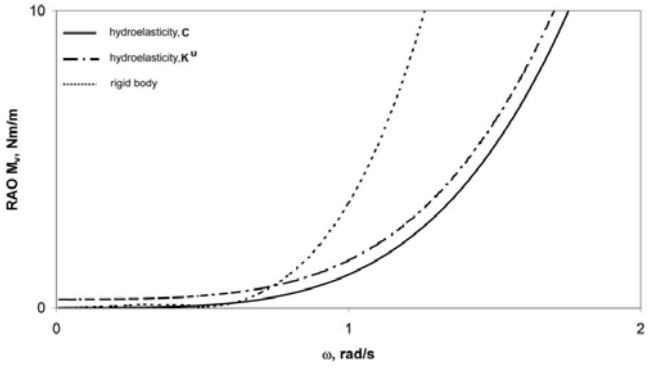

Figure 14 **Zoomed transfer function of vertical bending moment**
Slika 14 **Detalj prijenosne funkcije vertikalnog momenta savijanja**

10 Conclusion

The paper tends to shed more light on still open and challenging problem of restoring stiffness constitution in hydroelastic analysis of marine structures. Usually, restoring stiffness has to be taken into account together with geometric stiffness. Due to some equivalent parts, in this paper they are assembled in a physically transparent manner. Its simplified formulation is identical to one shown in [9], which is derived in a direct way under some assumptions.

Consistency of the unified geometric and restoring stiffness is checked by analytical solution for prismatic pontoon and satisfying of the rigid body equilibrium, well-known in the ship hydrostatics. Analytical formulae offer the possibility to follow physical background of each constitutive part and their mutual interference.

Derived theory application is illustrated in case of a segmented barge, for which the experimental data are available. It is shown that basic condition for each restoring stiffness formulation is convergence of elastic response to zero, as the wave frequency approaches to zero value. Both the analytical solution of the pontoon unified geometric and restoring stiffness and numerical example of the segmented barge can be used as benchmark in hydroelastic analysis of marine structures as in, for instance, [26].

Geometric stiffness can be decomposed into three parts, one imposed by gravity in vertical direction, another by hydrostatic pressure and the third one dependent on curvature. The former is included in the ordinary restoring stiffness, so that in case of small axial and transverse contribution it is possible to operate with ordinary restoring stiffness without geometric stiffness. Such situation occurs in ships with low still water stress distribution. If ship hydroelastic analysis is handled with geometric stiffness included, then the additional axial stress caused by resistance and trust can also be taken into account.

The geometric stiffness has to be accounted for in hydroelastic analysis of slender structures, like floating airports and tension leg platforms. In the former case, geometric stiffness reduces the total structure stiffness due to compression, while in the latter case it is increased like in the strings of musical instruments. Small equilibrium disturbance at zero wave frequency, which occurs if geometric stiffness is included, should be further investigated.

An advantage of applying unified geometric and restoring stiffness in any case is a possibility to generate geometric stiffness by standard procedure in the most commercial FEM packages for structural analysis. Thus, only integration over wetted surface remains to be additionally done within the modal superposition method. Otherwise, the calculation of gravity stiffness should be performed by integration per structure volume, and that could present a complex problem. If geometric stiffness is included in hydroelastic analysis, then dry natural vibrations can be calculated with the complete structural stiffness. In that case one step of modal superposition calculation is avoided.

One of the further tasks in hydroelastic analysis of marine structures is just surface integration itself, and finding the way how to overcome the gap between the structural FEM mesh and panel net of wetted surface. Also, the application of the presented theory for a rational and reliable hydroelastic analysis of a large container ship is an additional challenging task.

The advanced restoring stiffness formulation with geometric stiffness included, Eq. (2), is not yet generally accepted among hydrodynamics experts, since for them it seems strange that structure participates in hydro-mechanical resistance. The structure is expected to be involved only in the conventional stiffness. By formulating the unified geometric and restoring stiffness and its simplification, identical to Eq. (2), in a more transparent way in this self-contained paper, with detailed analytical consideration in case of a prismatic pontoon and segmented barge, this avoidance could be overcome.

Acknowledgment

The investigation has been carried out within the national project of the Croatian Ministry of Science, Education and Sports entitled: Load and Response of Ship Structures and the EU FP7 Project TULCS (Tools for Ultra Large Container Ships). The authors express their gratitude to Stipe Tomašević, PhD, FAMENA, University of Zagreb, for numerical calculation of the barge hydroelastic response.

References

[1] RINA, 2008, 'Design and Operations of Container Ships', London.
[2] PAYER, H.: 'Technological and Economic Implications of Mega-Container Carriers', SNAME Transactions, 2001, Vol. 109, p. 101-120.

[3] SENJANOVIĆ, I., MALENICA, Š., TOMAŠEVIĆ, S.: 'Investigation of Ship Hydroelasticity', Ocean Eng., 2008, 35, p. 523-535.
[4] BISHOP, R. E. D., PRICE, W. G.: 'Hydroelasticity of Ships', Cambridge University Press, 1979.
[5] SENJANOVIĆ, I., TOMIĆ, M., TOMAŠEVIĆ, S.: 'An Explicit Formulation for Restoring Stiffness and Its Performance in Ship Hydroelasticity', Ocean Eng., 2008, 35, p. 1322-1338.
[6] PRICE, W.G., WU, Y.: 'Hydroelasticity of Marine Structures', Theoretical and Applied Mechanics, Elsevier Science Publishers B.V., 1985, p. 311-337.
[7] NEWMAN, J. N.: 'Wave Effects on Deformable Bodies', Appl. Ocean Res. 1994, 16, p. 47-59.
[8] RIGGS, H. R.: 'Hydrostatic Stiffness of Flexible Floating Structures', Proceedings of the International Workshop on Very Large Floating Structures, Hayama, Japan, 1996, p. 229-239.
[9] HUANG, L. L., RIGGS, H. R.: 'The Hydrostatic Stiffness of Flexible Floating Structures for Linear Hydroelasticity', Mar. Struct., 2000, 13, p. 91-106.
[10] MALENICA, Š.: 'Some Aspects of Hydrostatic Calculations in Linear Seakeeping', Proceedings of the 14th NAV Conference, 2003, Palermo, Italy.
[11] MALENICA, Š., MOLIN, B., REMY, F., SENJANOVIĆ, I.: 'Hydroelastic Response of a Barge to Impulsive and Non-ImpulsiveWave Loads', Proceedings of Hydroelasticity in Marine Technology, 2003, p. 107-115.
[12] KREYSZIG, E.: 1993, 'Advanced Engineering Mathematics', Wiley.
[13] SENJANOVIĆ, I., TOMAŠEVIĆ, S., VLADIMIR, N., TOMIĆ, M., MALENICA, Š.: 'Ship Hydroelastic Analysis with Sophisticated Beam Model and Consistent Restoring Stiffness', Hydroelasticity in Marine Technology, 2009, University of Southampton, p. 69-80.
[14] RIGGS, H.R.: 'Comparison of Formulations for the Hydrostatic Stiffness of Flexible Structures', Journal of Offshore Mechanics and Arctic Engineering, 2009, Vol. 131/024501.
[15] ALFIREVIĆ, I.: 'Introduction to Continuum Mechanics', Golden Marketing, Zagreb, 2003, (in Croatian).
[16] ZIENKIEWICZ, O.C.: 'The Finite Element Method in Engineering Science', McGraw-Hill, 1971, London.
[17] SORIĆ, J.: 'The Finite Element Method', Golden marketing – Tehnička knjiga, 2004, Zagreb (in Coatian).
[18] HOLAND, J., BELL, K.: 'Finite Element Methods in Stress Analysis', Tapir, 1970.
[19] SENJANOVIĆ, I.: 'Finite Element Method in Ship Structures', University of Zagreb, 1998, Zagreb (in Croatian).
[20] SZILARD, R.: 'Theories and Application of Plate Analysis', Wiley, 2004.
[21] SNAME, 'Principles of Naval Architecture', Jersey City, 1988.
[22] SENJANOVIĆ, I., ĆATIPOVIĆ, I., TOMAŠEVIĆ, S.: 'Coupled Horizontal and Torsional Vibrations of a Flexible Barge', Engineering Structures 30, 2008, p. 93-109.
[23] REMY, F., MOLIN, B., LEDOUX, A.: 'Experimental and Numerical Study of the Wave Response of a Flexible Barge', Hydroelasticity in Marine Technology, 2006, Wuxi, China, p. 255-264.
[24] TOMAŠEVIĆ, S.: 'Hydroelastic Model of Dynamic Response of Container Ships in Waves', Ph.D. Thesis, FAMENA, 2007, University of Zagreb, Zagreb (in Croatian).
[25] Bureau Veritas, 'HYDROSTAR, User's Manual', 2006, Paris.
[26] RIGGS, H.R., NIIMI K.M., HUANG, L.L.: 'Two benchmark problems for three-dimensional linear hydroelasticity', Journal of Offshore Mechanics and Arctic Engineering, Vol. 129, 2007.

Appendix A Formulation of normal vector directional derivative

Within continuum mechanics, the following relation between the actual and the referent differential surface exists [15]:

$$d\tilde{\mathbf{S}} = \left|\mathbf{F}\right|(\mathbf{F}^{-1})^T\, dS, \tag{A1}$$

where F is the deformation gradient matrix, which in the case of the displacement vector **H** takes the form

$$\mathbf{F} = \begin{bmatrix} 1+\dfrac{\partial H_x}{\partial x} & \dfrac{\partial H_x}{\partial y} & \dfrac{\partial H_x}{\partial z} \\ \dfrac{\partial H_y}{\partial x} & 1+\dfrac{\partial H_y}{\partial y} & \dfrac{\partial H_y}{\partial z} \\ \dfrac{\partial H_z}{\partial x} & \dfrac{\partial H_z}{\partial y} & 1+\dfrac{\partial H_z}{\partial z} \end{bmatrix}. \tag{A2}$$

Thus, for the directional derivative of normal vector one can write

$$D_H(\mathbf{n}) = \frac{d\tilde{\mathbf{S}} - d\mathbf{S}}{\left|d\mathbf{S}\right|} = \left(\left|\mathbf{F}\right|(\mathbf{F}^{-1})^T - \mathbf{I}\right)\mathbf{n}, \tag{A3}$$

where **I** is the unit matrix and **n** is the unit normal vector. The inversion of matrix **F** and its transpose, after neglecting the small terms of higher order, lead to the following formula

$$\begin{aligned} D_H(\mathbf{n}) = &\left[\left(\frac{\partial H_y}{\partial y}+\frac{\partial H_z}{\partial z}\right)n_x - \frac{\partial H_y}{\partial x}n_y - \frac{\partial H_z}{\partial x}n_z\right]\mathbf{i} \\ &+\left[-\frac{\partial H_x}{\partial y}n_x + \left(\frac{\partial H_x}{\partial x}+\frac{\partial H_z}{\partial z}\right)n_y - \frac{\partial H_z}{\partial y}n_z\right]\mathbf{j} \\ &+\left[-\frac{\partial H_x}{\partial z}n_x - \frac{\partial H_y}{\partial z}n_y + \left(\frac{\partial H_x}{\partial x}+\frac{\partial H_y}{\partial y}\right)n_z\right]\mathbf{k} \end{aligned} \tag{A4}$$

Eq. (A4) can also be presented in the vector notation if the contents within the box brackets are extended and subtracted with the terms $\frac{\partial H_x}{\partial x}n_x$, $\frac{\partial H_y}{\partial y}n_y$ and $\frac{\partial H_z}{\partial z}n_z$, respectively. This leads to

$$D_H(\mathbf{n}) = \mathbf{n}(\nabla\mathbf{H}) - \left[\left(\mathbf{n}\frac{\partial\mathbf{H}}{\partial x}\right)\mathbf{i} + \left(\mathbf{n}\frac{\partial\mathbf{H}}{\partial y}\right)\mathbf{j} + \left(\mathbf{n}\frac{\partial\mathbf{H}}{\partial z}\right)\mathbf{k}\right] \tag{A5}$$

Appendix B Integral matrices

In the hydroelastic analysis of barge as a beam, one is faced with typical integral matrices (76) and (86), which can be solved analytically for the analytical natural modes, Eqs. (81) and (82). The first matrix is diagonal due to orthogonality of the natural modes

$$I_{nn}^{(0)} = \int_{-l}^{l} w_n^2 \mathrm{d}x = \frac{l}{4}\left[\frac{1}{\cosh^2\beta_n l} + \frac{3}{\beta_n l}\left(\mathrm{tgh}\beta_n l + \mathrm{tg}\beta_n l\right) + \frac{1}{\cos^2\beta_n l}\right], \quad n = 2,4,... \tag{B1}$$

where the second term represents the frequency equation equal to zero [22]. That leads to the value

$$I_{nn}^{(0)} = \frac{l}{2}, \tag{B2}$$

which is also valid for anti-symmetric elastic modes. In a similar way the other two integral matrices can be determined, too. Numerical values of the integral matrices and the boundary value matrix are listed in Tables B1-B4, respectively. Matrix $\mathbf{I}^{(2)}$ is also diagonal due to orthogonality of the natural modes.

Table B1 **Integral matrix, $\mathbf{I}^{(0)}$**
Tablica B1 **Matrica integrala, $\mathbf{I}^{(0)}$**

2.445					
	1.218				
		0.611			
			0.612		
				0.613	
					0.612

Table B2 **Integral matrix, $\mathbf{I}^{(1)}$**
Tablica B2 **Matrica integrala, $\mathbf{I}^{(1)}$**

0.000	0.000	0.000	0.000	0.000	0.000
0.000	2.445	0.000	2.000	0.000	2.000
0.000	0.000	5.059	0.000	3.617	0.000
0.000	2.000	0.000	11.159	0.000	5.897
0.000	0.000	3.617	0.000	19.160	0.000
0.000	2.000	0.000	5.897	0.000	29.133

Table B3 **Integral matrix, $\mathbf{I}^{(2)}$**
Tablica B3 **Matrica integrala, $\mathbf{I}^{(2)}$**

0.000					
	0.000				
		8.562			
			65.186		
				250.765	
					683.829

Table B4 **Boundary value matrix** $\left[\left(w_i\varphi_j\right)_{-l}^{l}\right]$
Tablica B4 **Matrica rubnih vrijednosti** $\left[\left(w_i\varphi_j\right)_{-l}^{l}\right]$

0.000	0.000	3.801	0.000	9.008	0.000
0.000	2.445	0.000	7.868	0.000	14.143
0.000	0.000	3.801	0.000	9.008	0.000
0.000	2.000	0.000	6.436	0.000	11.569
0.000	0.000	3.801	0.000	9.008	0.000
0.000	2.000	0.000	6.436	0.000	11.569

By knowing the basic matrices, the constitutive barge stiffness and mass matrices can be determined. It is obvious that asymmetry of the restoring stiffness **C** is caused by asymmetry of the boundary matrix, Table B4. Also, the unified geometric and restoring stiffness matrix can be calculated according to Eq. (77).